S21 Physics of Complex Systems
Física de Sistemas Complejos (GEFENOL)

13/07 Wednesday afternoon, Aula 1.2

15:30-16:00 V. Martín Mayor
The mystery of rejuvenation and memory in spin-glasses

16:00-16:15 J. Moreno Gordo
Temperature Chaos is present in off-equilibrium spin-glass dynamics

16:15-16:30 J. Cantisán Gómez
Stochastic Resetting in the Kramers problem

16:30-16:45 R. Gutiérrez
Finding generalized optimal paths and unveiling dynamical phase transitions through the large deviations of random walks on graphs

16:45-17:00 J. Borondo
Forecasting Fruits and Vegetable Prices: Reservoir computing outperforms traditional methods and neural networks

17:00-17:15 R. A. Rica
Brownian dynamics of interacting particles confined in an aqueous Paul trap

17:15-17:45 **Coffee Break**

17:45-18:15 J. García-Ojalvo
Temporal oscillations as spatial organizers in multicellular populations

18:15-18:30 M. Sireci
A macroecological law of species interactions in microbial ecosystems

18:30-18:45 J. Fernández-Gracia
Inferring Generalized Lotka-Volterra parameters from longitudinal microbial data

18:45-19:00 G. I. Triguero Platero
From microscopics to macroscopic hydrodynamics of collective cell motion

19:00-19:15 V. Buendía
The excitatory-inhibitory branching process: a parsimonious view of cortical asynchronous states, excitability, and criticality

19:15-19:30 E. Abad
Normal and anomalous diffusion in evolving domains: a brief overview of some recent results

S21 Physics of Complex Systems
Física de Sistemas Complejos (GEFENOL)

14/07 Thursday afternoon, Aula 1.2

15:30-16:00 M. Castro
The turning point and end of an expanding epidemic cannot be precisely forecast

16:00-16:15 P. Carpena
Contagion effect in exams

16:15-16:30 P. I. Hurtado
Building continuous time crystals from rare events

16:30-16:45 J. C. Losada
Multipolarity in a Complex Society

16:45-17:00 M. Grande
Evolutionary Dynamics of the Ethereum Transaction Network

17:00-17:15 R. Toral
Numerical sampling rare of rare trajectories using stochastic bridges

17:15-17:45 **Posters and Coffee**

17:45-18:15 O. Agam
"Aging" and slow relaxation in the dynamics of living cells

18:15-18:30 J. M. Marcos
Optimal control of bidirectional escape from a symmetric potential well

18:30-18:45 A. Domínguez
Colloidal monolayers: bridging the gap between two and three spatial dimensions

18:45-19:00 P. Maynar
Kinetic theory of fluids under strong confinement

19:00-19:15 A. Patrón
Optimal thermalisation for a generic d-dimensional harmonic oscillator

19:15-19:30 C. Pérez-Espigares
Direct evaluation of large deviations in open quantum systems

Posters:

11 A. V. Coronado
Nonlinearity test for complex time series

12 S. Martín-Gutiérrez
Statistical models of social interaction

13 M. I. García de Soria
Dynamics of hard particles confined by an isotropic harmonic potential

14 B. Skadden
Variability of spreading rate in forced plumes

15 I. González-Adalid
Accelerating out-of-equilibrium critical dynamics via magnetic domains

Two lines of space reserved to include
codes of the symposium and of this communication

The mystery of rejuvenation and memory in spin-glasses

Víctor Martín-Mayor[1]

[1] *Departamento de Física Teórica, Universidad Complutense, 28040 Madrid, Spain.*

*e-mail: presenting.authorB@murc.ia

The idea that theoretical physicists could build computers specifically designed to solve their problems, among other examples, has germinated in the Italian/Spanish Janus collaboration. Indeed, the Janus I [1] and Janus II [2] supercomputers deliver since 2008 the highest computing power Worldwide for spin-glasses simulations. The Janus collaboration is formed by researchers from the Universities of Zaragoza, Extremadura-Badajoz, Complutense de Madrid, La Sapienza-Roma and Ferrara, and is very proud to count Giorgio Parisi as a distinguished member.

The main focus of the talk will be describing our recent success in reproducing in a simulation using Janus II the spectacular memory and rejuvenation effects of spin glasses. Although memory and rejuvenation were discovered experimentally more than 20 years ago [3], convincingly reproducing these effects in a simulation seemed hopeless until now, and for very good reasons. Indeed, many pieces of the puzzle had to be gathered. First, we have needed to learn how to quantitatively extract the spin-glass coherence length (i.e. the size of the glassy domains) from simulations of non-equilibrium spin glass dynamics [4]. Second, one needs to reach reasonably large coherence lengths in the simulation, a task that demands the tremendous computing power of Janus II. A third step has been learning how to extrapolate from the numerical time and length scales to the experimental ones [5]. Fourth, Janus II has provided a crucial understanding about how temperature chaos in non-equilibrium dynamics really is [6]. These milestones have made possible undertaking a nice collaboration with the group of Ray Orbach in Texas. The collaboration with the Texan group has taught us how to perform in Janus II true çomputer experiments", in which the very same quantities are computed in the simulation and measured in a CuMn single crystal, and analyzed in a parallel way [7,8]. In fact, the 2022 temperature-chaos experiment by Orbach and Zhai [9] has produced crucial quantitative input to set up a successful simulation of memory and rejuvenation. A big surprise (at least surprising for us) is our finding that no less than three quite distinct length scales control aging dynamics [10].

[1] F. Belleti et al. (Janus Collaboration), *Commm. Phys. Comm.* **178**, 208 (2008).
[2] M. Baity-Jesi et al. (Janus Collaboration), *Commm. Phys. Comm.* **185**, 550 (2014).
[3] J. Jonason, E. Vincent, J. Hammann, J. P. Bouchaud, P. M. and Nordblad *Phys. Rev. Lett.* **81**, 3243 (1998).
[4] F. Belleti et al. (Janus Collaboration), *Phys. Rev. Lett.* **101**, 157201 (2008).
[5] M. Baity-Jesi et al. (Janus Collaboration), *Phys. Rev. Lett.* **120**, 267203 (2018).
[6] M. Baity-Jesi et al. (Janus Collaboration), *Communication Physics* **4**, 74 (2021).
[7] Q. Zhai, et al. (Janus collaboration), *Phys. Rev. Lett.* **125**, 237202 (2020).
[8] I. Paga et al. (Janus collaboration), *JSTAT* **2021**, 033301 (2021).
[9] Q. Zhai and R. Orbach, *Phys. Rev. B* **105**, 014434 (2022).
[10] M. Baity-Jesi et al. (Janus Collaboration), manuscript in preparation (2022).

Two lines of space reserved to include
codes of the symposium and of this communication

Temperature chaos is present in off-equilibrium spin-glass dynamics.

Marco Baity-Jesi,[1] Enrico Calore,[2] Andrés Cruz,[3,4] Luis Antonio Fernandez,[5,4] José Miguel Gil-Narvion,[4] Isidoro Gonzalez-Adalid Pemartin,[5] Antonio Gordillo-Guerrero,[6,7,4] David Iñiguez,[4,8,3] Andrea Maiorano,[9,10,4] Enzo Marinari,[11,10] Víctor Martin-Mayor,[5,4] Javier Moreno-Gordo,[7,4,*] Antonio Muñoz-Sudupe,[5,4] Denis Navarro,[12] Ilaria Paga,[13,5] Giorgio Parisi,[11,10] Sergio Perez-Gaviro,[14,4,3] Federico Ricci-Tersenghi,[11,10] Juan Jesús Ruiz-Lorenzo,[15,7,4] Sebastiano Fabio Schifano,[16] Beatriz Seoane,[5,4] Alfonso Tarancon,[3,4] Raffaele Tripiccione,[2] and David Yllanes[17,4]
(Janus Collaboration)

[1] *Eawag, Überlandstrasse 133, CH-8600 Dübendorf, Switzerland*
[2] *Dipartimento di Fisica e Scienze della Terra, Università di Ferrara e INFN, Sezione di Ferrara, I-44122 Ferrara, Italy*
[3] *Departamento de Física Teórica, Universidad de Zaragoza, 50009 Zaragoza, Spain*
[4] *Instituto de Biocomputación y Física de Sistemas Complejos (BIFI), 50018 Zaragoza, Spain*
[5] *Departamento de Física Teórica, Universidad Complutense, 28040 Madrid, Spain*
[6] *Departamento de Ingeniería Eléctrica, Electrónica y Automática, U. de Extremadura, 10003, Cáceres, Spain*
[7] *Instituto de Computación Científica Avanzada (ICCAEx), Universidad de Extremadura, 06006 Badajoz, Spain*
[8] *Fundación ARAID, Diputación General de Aragón, 50018 Zaragoza, Spain*
[9] *Dipartimento di Biotecnologie, Chimica e Farmacia, Università degli studi di Siena, 53100, Siena, Italy*
[10] *INFN, Sezione di Roma 1, I-00185 Rome, Italy*
[11] *Dipartimento di Fisica, Sapienza Università di Roma, and CNR-Nanotec, I-00185 Rome, Italy*
[12] *Departamento de Ingeniería, Electrónica y Comunicaciones and I3A, U. de Zaragoza, 50018 Zaragoza, Spain*
[13] *Dipartimento di Fisica, Sapienza Università di Roma, INFN, Sezione di Roma 1, I-00185 Rome,Italy*
[14] *Centro Universitario de la Defensa, 50090 Zaragoza, Spain*
[15] *Departamento de Física, Universidad de Extremadura, 06006 Badajoz, Spain*
[16] *Dipartimento di Scienze Chimiche e Farmaceutiche, Università di Ferrara e INFN Sezione di Ferrara, I-44122 Ferrara, Italy*
[17] *Chan Zuckerberg Biohub, San Francisco, CA, 94158, United States*

* jmorenogordo@gmail.com

Stochastic resetting in the Kramers problem

Julia Cantisán[1,*], Jesús M.Seoane[1], Miguel A. F. Sanjuán[1,2]

[1] *Nonlinear Dynamics, Chaos and Complex Systems Group, Departamento de Física, Universidad Rey Juan Carlos. Tulipán s/n, 28933 Móstoles, Madrid, Spain*
[2] *Department of Applied Informatics, Kaunas University of Technology Studentu 50-415, Kaunas LT-51368, Lithuania.*

*e-mail: julia.cantisan@urjc.es

The theory of stochastic resetting (SR) asserts that restarting a search process at certain times may accelerate the finding of a target. SR was first studied by Evans and Majumdar [1], who showed that the mean first passage time (MFPT) of a diffusing particle searching for a target in an infinite domain presents a minimum for a certain value of the resetting rate. Some natural processes such as animal foraging or human visual search utilize this mechanism to reduce the search time.

We study stochastic resetting as a strategy to reduce the escape time of a classical diffusing particle trapped in a potential well, which may escape due to thermal fluctuations, i.e., the Kramers problem [2]. This is equivalent to a search process where the target is the top of the energy barrier. We use a Monte Carlo approach, which is necessary for generic complex potentials. We demonstrate that this approach is in agreement with some analytical results and that this technique allows to explore the system in a different way.

We apply two resetting strategies: resetting at deterministic times (see Figure 1) and resetting at exponentially distributed times (treating the resetting events as Poisson events). We find that trajectories whose initial position corresponds to at least a 41% of the height of the potential barrier, show a minimum in the MFPT. For resetting at deterministic times, the best resetting strategy can be predicted in advance as the optimal resetting time interval is related to the wave pattern of first passage times found for the no resetting case.

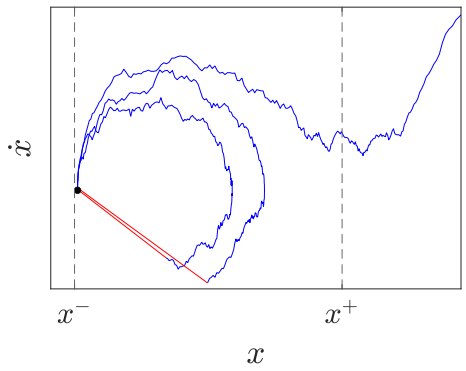

Figure 1. Phase space for a trajectory with deterministic resetting. The vertical dotted lines denote the edges of the potential well. The black point marks the initial condition, which is also the reset position. The trajectory moves around freely diffusing in the potential landscape until at $t = t_r$, the particle is immediately reset. This bit is marked in red. After two resetting events, the particle escapes.

[1] Martin R. Evans and Satya N. Majumdar, *Phys. Rev. Lett.* **106**, 160601 (2011).
[2] Julia Cantisán, Jesús M. Seoane and Miguel A.F. Sanjuán, *Chaos, Solitons and Fractals* **152**, 111342 (2021).

Acknowledgements: This work has been supported by the Spanish State Research Agency (AEI) and the European Regional Development Fund (ERDF, EU) under Projects No. FIS2016-76883-P and No. PID2019-105554GB-I00.

Two lines of space reserved to include
codes of the symposium and of this communication

Finding generalized optimal paths and unveiling dynamical phase transitions through the large deviations of random walks on graphs

Ricardo Gutiérrez[1,*] and Carlos Pérez-Espigares[2,3]

[1] *Grupo Interdisciplinar de Sistemas Complejos, Departamento de Matemáticas, Universidad Carlos III de Madrid, Spain.* [2] *Departamento de Electromagnetismo y Física de la Materia, Universidad de Granada, Spain.* [3] *Institute Carlos I for Theoretical and Computational Physics, Universidad de Granada, Spain.*

*e-mail: rigutier@math.uc3m.es

In a statistical mechanical formalism of ensembles of trajectories, dynamical large-deviation functions play a role analogous to that of thermodynamic potentials in equilibrium statistical mechanics. This is a powerful approach that has lately illuminated many aspects of non-equilibrium statistical physics. In fact, it can still yield novel perspectives and applications even in the analysis of such a simple process as a random walk on a graph, as we will see.

First we will illustrate how large-deviation functions of random walks can be employed for finding optimal paths and weight distributions in disordered discrete media such as random graphs and complex networks of different kinds, including spatial networks [1]. It is well known that many problems of theoretical and practical interest are related to finding shortest (or otherwise optimal) paths in networks, frequently in the presence of some obstacles or constraints. Another related sets of problems focus on optimal distributions of weights which, for a given connection topology, maximize some kind of flow or minimize a given cost function. In contrast to standard graph-theoretical methods, in our approach the paths are not limited to shortest paths and the weights must not necessarily optimize a given function. They can in fact be tailored to a given statistics of a time-integrated observable, which may be an activity or current, or local functions marking the passing of the random walker through a given node or link. This allows for great flexibility in the definitions of such generalized optimal paths and weight distributions. We illustrate this idea with an exploration of optimal paths in the presence of obstacles, and networks that optimize flows under constraints on local observables.

The study of optimal weight distributions in spatial networks contained in Ref. [1] shows intriguing localized vortex dynamics in random walks, similar to those that have been observed in the presence of exclusion effects [2]. To clarify this behavior, a more detailed study has been performed based on the two-dimensional random walk conditioned on partial currents, which reveals the existence of a dynamical phase transition between delocalized band dynamics and localized vortex dynamics [3]. We present a numerical microscopic characterization of the phases involved, and provide analytical insight based on the macroscopic fluctuation theory. The continuous phase transition is accompanied by spontaneous $\mathbb{Z}_2$-symmetry breaking whereby the stationary solution loses the reflection symmetry of the generator. Dynamical phase transitions similar to this one, which do not rely on exclusion effects or interactions, are expected to be observed in more complex non-equilibrium physics models.

[1] R. Gutiérrez and C. Pérez-Espigares, *Phys. Rev. E* **103**, 022319 (2021).
[2] T. Bodineau, B. Derrida, and J. L. Lebowitz, *J. Stat. Phys.* **131**, 821 (2008).
[3] R. Gutiérrez and C. Pérez-Espigares, *Phys. Rev. E* **104**, 044134 (2021).

Forecasting Fruits and Vegetable Prices: Reservoir computing outperforms traditional methods and neural networks

L.Domingo[1,2,3], M. Grande[3,4], F. Borondo[1,2], J. Borondo[4,5,*]

[1]*Instituto de Ciencias Matemáticas (ICMAT); Campus de Cantoblanco UAM; Nicolás Cabrera, 13-15; 28049 Madrid, Spain.*
[2]*Departamento de Química; Universidad Autónoma de Madrid; CANTOBLANCO - 28049 Madrid, Spain.*
[3]*Grupo de Sistemas Complejos; Universidad Politécnica de Madrid; 28035 Madrid, Spain.*
[4]*AgrowingData; Navarro Rodrigo 2 AT; 04001 Almería, Spain.*
[5]*Departamento de Gestión Empresarial; Universidad Pontificia de Comillas ICADE; Alberto Aguilera 23; 28015 Madrid, Spain.*

*e-mail: jborondo@gmail.com

The main goal of this work is to study the performance of reservoir commuting (RC) [1] based algorithms to predict the evolution of the prices of fruits and vegetables. Anticipating the prices is extremely important as their high volatility makes it difficult for farmers and coops to efficiently market the products. In fact, year in and year out we observe price crises where the commercialization of the product is not profitable, resulting in tons of waste of food. One of the challenges of this time series is that it has few training samples. In addition, the European market is a connected network where prices are influenced by hundreds of factors, such as exports & climate. Thus, we also provide external variables that capture this information to the algorithms to obtain more accurate results. RC is especially useful in this setting, since it uses both the past value of the time series and regressor variables to extrapolate the time series. Moreover, its simple training framework reduces the chances of overfitting the training data. We assess the performance of five RC models and compare the results with two benchmark time series models: a Long-Short Term Memory neural network (LSTM) [2] and a Seasonal Autoregressive Integrated Moving Average (SARIMA) [2].

We have trained the five RC models and the two benchmark models, and evaluated their performance in the test set. Figure 1 shows the prediction of the seven models compared with the true values of the prices' time series. To quantify and compare the performance of the models, we have used several metrics including the mean absolute error (MAE). Our results show clearly that the configurations based on RC outperform both SARIMA and LSTM.

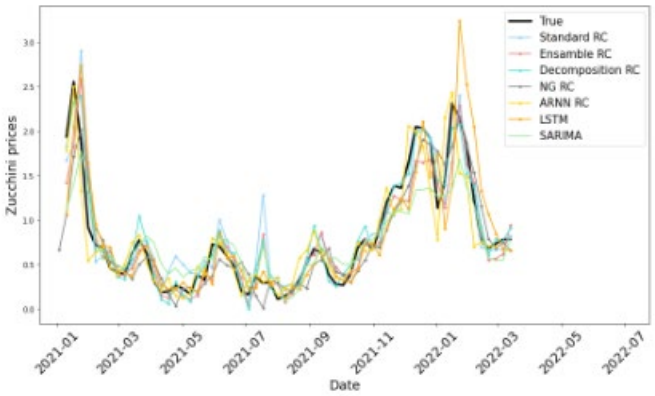

Figure 1. Prediction of the time evolution for the test set of the seven machine learning models studied in this work, together with the real time series.

[1] R. Gao, L. Du, O. Duru, and K. F. Yue , Time series forecasting based on echo state network and empirical wavelet transformation, Appl. Soft Comput **102**, 107111 (2021).
[2] S. Hochreiter and J. Schmidhuber, Long short-term memory, *Neural Comput.* **9**, 1735 (1997).
[3] P. Chen, A. Niu, D. Liu, W. Jiang, and B. Ma, Time series forecasting of temperatures using sarima: An example from nanjing, *IOP Conference Series: Materials Science and Engineering* **394**, 052024 (2018).

Two lines of space reserved to include
codes of the symposium and of this communication

Brownian dynamics of interacting particles confined in an aqueous Paul trap

Carlos D. González-Gómez[1,2], **Raúl A. Rica**[1,*]

[1] *Nanoparticles Trapping Laboratory, Department of Applied Physics, Universidad de Granada, Av. Fuentenueva s.n., 18071 Granada, Spain.*
[2] *Universidad de Málaga, Departamento de Física Aplicada II, Escuela de Ingenierías Industriales, 29071 Málaga, Spain.*

*e-mail: rul@ugr.es

The Brownian dynamics of *individual* microparticles in suspension can be studied in detail with optical tweezers, as it has been demonstrated in multiple situations [1–4]. Optical tweezers can also be used to simultaneously manipulate multiple particles in different potential wells, but the simultaneous trapping of multiple particles in a *single potential well* is not possible with this technique. Paul traps are able to store charged particles in a single potential well, leading to the formation of so-called Coulomb crystals [5]. Typical experiments are performed with ions in vacuum, where the particles interact via Coulomb repulsion. In a liquid, charged microparticles can still be trapped with Paul traps [6], but they have never been tested with multiple particles trapped together.

Here, we present a Paul trap that is able to trap tens of particles in a microfluidic device, which allows us to study the Brownian dynamics of interacting particles. Our Paul trap is composed of two gold microelectrodes deposited on borosilicate glass with ring geometry (see Fig. 1), and implemented together with an optical tweezers setup. This combination creates a hybrid trap [7] that provides us with enhanced manipulation capabilities. First, we characterize the trap by video-tracking the diffusion of a single particle in the potential well under different conditions, and also measuring the electric field within the Paul trap with help of the optical tweezers. Further, we track the trajectory of several particles simultaneously and extract information of their interactions from the analysis of their mean squared displacement using two types of polystyrene particles, one of which strongly polarize in presence of an AC electric field and thus tend to form particle chains. Finally, we discuss the prospects of such a device for fundamental studies of interacting Brownian particles in a potential well.

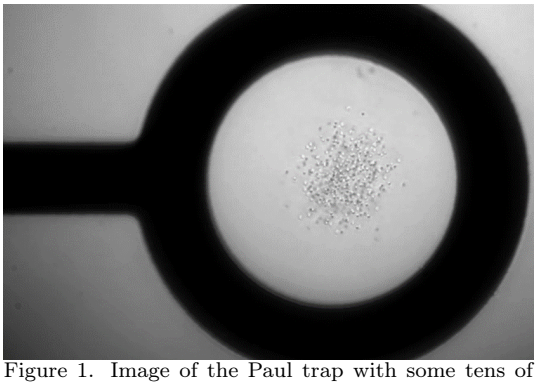

Figure 1. Image of the Paul trap with some tens of 1-μm polystyrene particles trapped together in liquid.

[1] J. Gieseler *et al.*, *Advances in Optics and Photonics* **13**, 74–241 (2021).
[2] I.A. Martínez, É. Roldán, L. Dinis, & R.A. Rica, *Soft Matter*, **13**, 22–36 (2017).
[3] F. Ricci, R.A. Rica *et al.*, *Nature Communications*, **8**, 15141 (2017).
[4] A. Kumar & J. Bechhoefer, *Nature*, **584**, 64?-68 (2020).
[5] R.C. Thompson, *Contemporary Physics*, **56**, 63–79 (2015).
[6] W. Guan, S. Joseph, J.H. Park, P.S. Krstić, & M.A. Reed, *PNAS*, **108**, 9326-9330 (2011).
[7] G.P. Conangla, R.A. Rica & R. Quidant, *Nano Letters*, **20**, 6018-?6023 (2020).

Acknowledgements: The Authors acknowledge financial support from FEDER/Junta de Andalucía-Consejería de Transformación Económica, Industria, Conocimiento y Universidades/ Proyecto P18-FR-3583.

Temporal oscillations as spatial organizers in multicellular populations

Jordi Garcia-Ojalvo

Department of Medicine and Life Sciences, Universitat Pompeu Fabra, Parc de Recerca Biomèdica de Barcelona, Dr. Aiguader 88, 08003 Barcelona, Spain

*e-mail: jordi.g.ojalvo@upf.edu

Multicellular organisms rely on a careful spatiotemporal orchestration of form and function, covering multiple biological scales that range from molecules to cellular populations. Much current research is being devoted to understanding how space and time are integrated as organisms develop. In this talk I will address this issue in bacterial biofilms, multicellular populations with important clinical and environmental implications. Using a combination of experiments and computational modeling, I will show that oscillations in time, driven by molecular interactions, are transformed into periodicity in space, driven by cellular behavior, not unlike the segmentation clock that underlies somitogenesis in vertebrates. I will discuss the molecular mechanism underlying this phenomenon, and the biological function that this behavior might play in the life cycle of bacterial populations.

A macroecological law of species interactions in microbial ecosystems

M. Sireci[1,*],M.A. Muñoz[1], J.Grilli[3]

[1]*Departamento de Electromagnetismo y Física de la Materia e Instituto Carlos I de Física Teórica y Computacional. Universidad de Granada. E-18071, Granada, Spain* [2]*Quantitative Life Sciences, The Abdus Salam International Centre for Theoretical Physics, 34151 Trieste, Italy*

*e-mail: msireci@onsager.ugr.es

Microbial ecosystems are the archetype of complex systems: their stability, functionality and resilience are "macroscopic"properties emerging from very diverse species "microscopic interactions. These communities are diffused all across the biosphere, from the human gut to glaciers, from soil to activated sludge. Understanding common properties of such diverse communities can pave the way to elucidate the common mechanisms behind the emergence of interactions and coexistence. The question of how coexistence of species is generated and maintained is as old as ecology itself. Many ecological "forces" such as competition, cooperation, demographic fluctuation, environmental fluctuation and filtering, migration, predation etc. are expected to act together in ecosystems. Disentangling the effect and intensity of each of theses forces in natural communities is the focus of present research. Thanks to a recent revolution in the availability of high quality data, natural microbial ecosystems offer an invaluable possibility to tackle this question.Here, we explore if it is possible to discriminate a dominant force at a give resolution of genetic similarity. Indeed, shedding light on how bacteria interact as function of their genetic similarity is extremely relevant both at fundamental and practical level, with consequences on human health. By using both relative-abundances and metagenomic data, we reveal the presence of a new macroecological law relating correlation and phylogenetic similarity. In particular, the average correlation of species abundance fluctuation ij decays with phylogenetic distance d ij from positive to null values following a stretch exponential function:

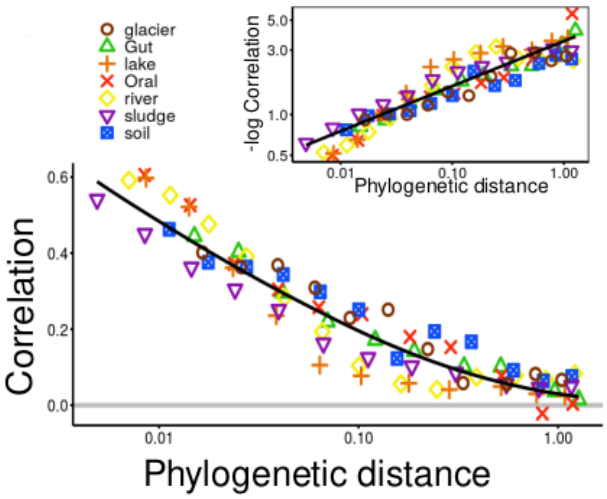

Figure 1. The correlation of abundance fluctuation averaged over all couples within a given discretized distance bin (colored symbols) decays with the phylogenetic distance (log scale). The black line is a stretched-exponential decay, where ≈ 3.5. To emphasize the functional dependence, the inset shows the same data but for the log of the correlations and in double logarithmic scale, i.e. a representation in which stretched exponential functions become straight lines; in this case with slope 1/3.

$$\eta_{ij} = e^{-\lambda d_{ij}^{1/3}},$$

consistently in all empirically analyzed biomes both across communities (hosts) and in temporal data for each community, see Fig. 1. By scrutinizing different ecological models, we show that competition cannot reproduce the observed pattern. Instead, the elucidated macroecological law is explained quantitatively by the "correlated stochastic logistic model" (CSLM) pointing to environmental filtering as the dominant ecological force at this resolution level. Finally we show that the macroecological law is valid also for temporal data of a single community, and that the properties of delayed temporal correlation are also reproduced by the CSLM. We conclude by arguing that in order to understand interactions in microbial ecosystems one needs to abandon the concept of species and study the system from different scales, much as done in physics exploiting renormalization group ideas.

Two lines of space reserved to include
codes of the symposium and of this communication

Inferring Generalized Lotka-Volterra parameters from longitudinal microbial data

Somaye Sheykhali[1], **Juan Fernández-Gracia**[1,*], Carlos J. Melián[1], Xabier Irigoien[2], Carlos M. Duarte[3], Víctor M. Eguíluz[1]

[1]*Instituto de Física Interdisciplinar y Sistemas Complejos IFISC (CSIC-UIB), Palma, Spain.* [2]*AZTI Tecnalia, Pasaia, Spain.* [3]*Red Sea Research Center (RSRC) and Computational Bioscience Research Center (CBRC), King Abdullah University of Science and Technology, Thuwal, Saudi Arabia*

*e-mail: juanf@ifisc.uib-csic.es

Microbial communities form the largest, more diverse and complex ecosystems on the planet. The interactions among their individuals are diverse, encompassing predation, mutualism, comensalism, amensalism or competition. Measuring these interactions in direction and strength at a large scale is a challenging process that requires a combination of data analysis and modeling. Furthermore, the dynamic nature of the abundances of different species of microorganisms cannot be ignored to present a sound theory on microbial interactions.

Data. We use experimental data that reported the OTU relative abundance – operational taxonomic units, which are quasi-equivalent to a species definition – every day for a period of 20 days in 5 different experiments, with 2 replicates for each. So, for each OTU i we have the relative abundance x_i^t for each $t = 1d, \ldots, 20d$.

Model. We will assume a Generalized Lotka-Volterra model to fit the data. The choice of this model is motivated by the power-law variation in OTU abundances, which suggests a multiplicative process. The model is defined by the following system of non-linear ordinary differential equations

$$\frac{1}{x_i}\frac{d}{dt}x_i = a_i + \sum_{j=1}^{N} \beta_{ij} x_j, \tag{1}$$

where N is the total number of OTUs considered. They consist of a local growth term and an interaction term that encodes the effect of other OTU abundances on the self abundance of one OTU. The particular values of β_{ij} as compared to βji let us define different types of interaction (predation when both have different sign, competition when both are negative, mutualism when both are positive, comensalism when one is positive and the other is 0 and amensalism when one is negative and the other is 0).

Parameter estimation. In order to estimate the best parameters that fit the data we minimize χ^2 assuming the model in Eq. (1). We assume that the fitting is to $\frac{1}{x_i}\frac{dx_i}{dt}$, which is approximated by $W_i^t = \frac{x_i^t - x_i^{t-1}}{x_i^{t-1}}$ from the data. The result of this minimization has the solution

$$a_i = \langle W_i \rangle - \beta_{ij}\langle x_j \rangle \quad \text{and} \quad \beta_{ij} = \Omega_{ik} C^{-1}_{kj}, \tag{2}$$

where $\Omega_{ij} = \langle W_i x_j \rangle - \langle W_i \rangle \langle x_j \rangle$, C^{-1}_{kj} are the elements of the inverse of the covariance matrix ($C_{ij} = \langle x_i x_j \rangle - \langle x_i \rangle \langle x_j \rangle$) and the operator $\langle \cdot \rangle$ denotes the average over all time points. We apply a regularization method to avoid overfitting.

Results. The results of the fitting procedure let us explore the parameters that best fit the data. We find that the fixed points defined by these parameters do not correspond to feasible configurations of the model. We also explore the different types of interactions that are present in the system. Neutral and non-reciproval (commensalist and amensalist) dominate, while reciprocal interactions account for a small percentage of the interactions. These results are statistically significant when compared to randomizations of the interaction matrices.

Discussion. The fitted model reveals thus the intrinsic growth rates and the interaction network among OTUs. The estimated parameters imply fixed points that are not feasible, pointing to the fact that the dynamics might be operating around more complex attractors. The interaction types that dominate the results are non-reciprocated. These type of interactions have been mostly ignored in the modeling literature and deserve more attention for a proper description of microbial ecosystems.

Acknowledgements: We aknowledge funding from grant PID2020-114324GB-C22 funded by MCIN/AEI/10.13039/501100011033.

From microscopics to macroscopic hydrodynamics of collective cell motion

Gloria Irene Triguero Platero[1,*], Luis Bonilla [2], Falko Ziebert[1]

[1] *Institute for Theoretical Physics, Heidelberg University, GERMANY* [2] *Department of Mathematics, Universidad Carlos III de Madrid, SPAIN*

*e-mail: gloria.triguero_platero@stud.uni-heidelberg.de

Collective cell migration in a cellular monolayer has been studied extensively experimentally, and modelled with many different approaches. In this project, two of the most prominent ones have been developed and critically compared to each other: an Active Vertex Model (AVM) that describes the "microscopic"dynamics of each cell, and a coarse-grained macroscopic description via hydrodynamic variables, in which the monolayer is described as an anisotropic fluid consisting of deformable particles.

As evidenced in reference [1], including effective inertial effects is required in order to match experimental results. Therefore, we here have developed underdamped dynamics for both approaches. Comparing them is expected to shed light on how microscopic changes affect macroscopic behaviour.

The AVM describes the monolayer as a network of polygonal cells [2]. Its dynamics can be captured via the vertices of the polygons or the cell centers. It is possible to go from one description to the other due to the dual nature of the Delaunay triangulation, that connects cell centers, with the Voronoi tesselation, that defines the boundaries. The model is implemented in the *SAMoS* software [2]. The energy function of the system includes terms related to a preferred cell area and perimeter, and a line tension term for the cell-junctions. Then, the forces can be computed as $F_i = -\nabla_{\boldsymbol{r}_i}[E_{VM} + V_{soft}(|\boldsymbol{r}_i - \boldsymbol{r}_j|)]$, where a soft core repulsion has been added to avoid pathologically elongated cells [1]. An example of expanding cell monolayer can be seen in Figure [1].

We then want to obtain a continuum description of the model. In order to do so, we introduce continuum microscopic field variables and then coarse-grain them to get macroscopic variables and their hydrodynamics. We introduce a mass and momentum density $\hat{\rho}(\boldsymbol{x},t)$, $\hat{\boldsymbol{g}}(\boldsymbol{x},t)$, and add a shape tensor field as in reference [3], $\hat{G}^{\alpha}_{ij} = \frac{1}{n}\sum_{\mu=1}^{n} \Delta x_i^{\alpha\mu}\Delta x_j^{\alpha\mu}$.

The macroscopic fields $\phi = \rho$, $\boldsymbol{g}$ and G^{α}_{ij} corresponding to the microscopic fields $\hat{\phi}$ are defined via $\phi(\boldsymbol{x},t) = \int \hat{\phi}\,\mathcal{P}\prod_{\alpha} d\boldsymbol{v}_{\alpha} d\boldsymbol{x}_{\alpha}$ with $\mathcal{P}$ the probability density. The latter satisfies a Fokker-Planck equation, from which we obtain the equations of motion for the macroscopic variables. For long spatial scales compared to the cell size, we then extract the continuum limit of the hydrodynamic equations.

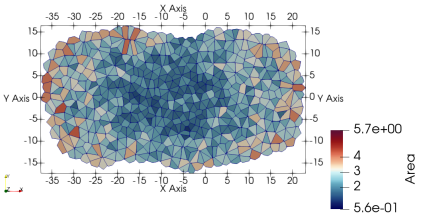

Figure 1. Expanding cell monolayer in which it can be seen that inner cells have smaller area than outer ones, as observed experimentally [1].

This project bears high biophysical relevance, both due to the system studied and to the bridge built between the AVM and its coarse-grained description. It will also allow to compare both models numerically in order to verify their consistency, and their agreement with experimental results.

[1] Luis L. Bonilla, Ana Carpio and Carolina Trenado, *PLOS Computational Biology* **16**, 1–43 (2020).
[2] Daniel L. Barton, Silke Henkes, Cornelis J. Weije, Rastko Sknepnek, *PLOS Computational Biology* **13**, 1005569 (2017).
[3] Arthur Hernandez and M. Cristina Marchetti, *Physical Review E* **103**, 032612 (2021).

The excitatory-inhibitory branching process: a parsimonious view of cortical asynchronous states, excitability, and criticality.

Roberto Corral López[1], **Victor Buendía**[2,*], Miguel A. Muñoz[1]

[1] *Dpto. de Electromagnetismo y Física de la Materia e Instituto Carlos I de Física Teórica y Computacional, Universidad de Granada. E-18071, Granada, Spain* [2] *Dpt. of Computer Science, University of Tübingen, and Max Planck Institute for Biological Cybernetics, Tübingen, 72076, Germany*

*e-mail: vbuendiar@onsager.ugr.es

The branching process is the minimal model for propagation dynamics, avalanches and criticality, broadly used in neuroscience. In this work we present a simple extension of it, adding inhibitory nodes, which induces a much-richer phenomenology, including a new phase. This novel phase is characterised by features not usually observed in typical active phases, such as constant levels of low activity – independently of the control parameters– and quasioscillations. Remarkably this new phase displays all the key features of "asynchronous states" in cortical networks, and captures a wealth of non-trivial features of spontaneous brain activity, such as collective excitability, hysteresis, tilted avalanche shapes, and partial synchronization, allowing us to rationalize striking empirical findings within a common parsimonious framework.

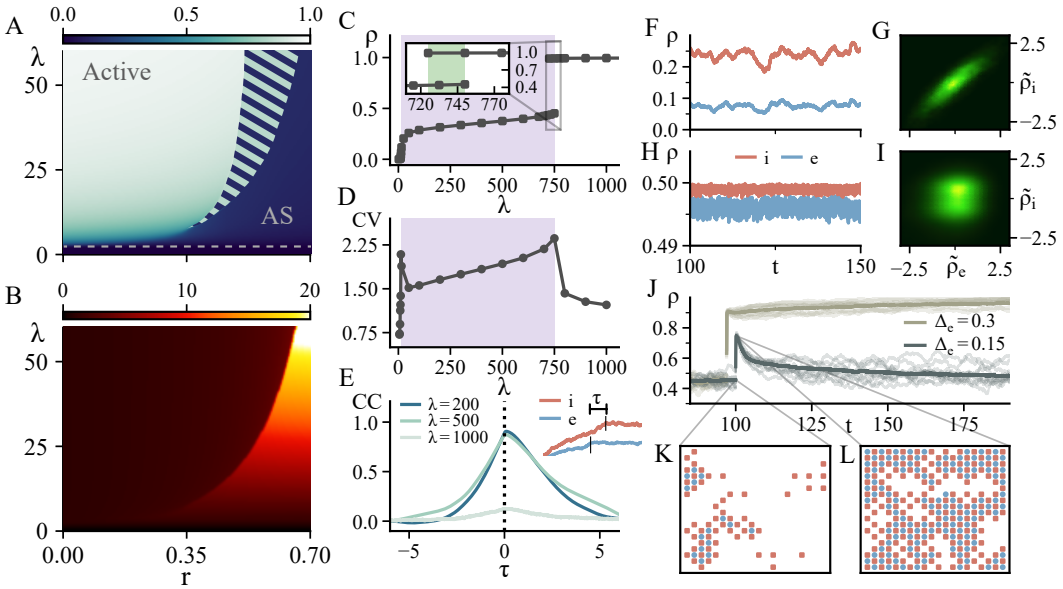

Figure 1. Features of the asynchronous phase. Parameters: λ, infection rate; r, inhibition strength; ρ, average activity (A-B) Analytical results for annealed random networks: (A) Stationary activity. Dashed line indicates the end of the quiescent phase and stripes signal the bistability region between the AI and active phases. (B) Henrici index gauging the level of excitability. (C-L) Results for a 2D lattice with $N = 10^4$. (C) Section of the phase diagram illustrating the discontinuous transition with bistability and (D) coefficient of variation (CV) for different values of λ (E) Lagged cross-correlations (CC) between excitatory and inhibitory time series; total excitatory and inhibitory activity as a function of time is plotted in (F) for the AS phase and in (H) for the standard active phase (G-I) same as in F and H, respectively, plotted normalized activities. (J) Stimulation experiment, where a fraction of excitatory nodes is transiently activated. In the bistability region, this can drive the system from the AS phase to the standard active phase. ($N = 20^2$).

[1] Corral, R. Buendía, V., and Muñoz, M.A., The excitatory-inhibitory branching process: a parsimonious view of cortical asynchronous states, excitability, and criticality. *Under review in Phys. Rev. Lett.* Arxiv: https://arxiv.org/abs/2203.16374 (2022).

Acknowledgements: We acknowledge the Spanish Ministry and Agencia Estatal de investigación project PID2020-113681GB-I00, the Consejería de Conocimiento, Investigación Universidad, Junta de Andalucía and European Regional Development Fund, project references A-FQM-175-UGR18 and P20-00173 for financial support. R.C.L. acknoledges funding from grant FPU19/03887. V.B. was supported by a Sofja Kovalevskaja Award from the Alexander von Humboldt Foundation.

Two lines of space reserved to include
codes of the symposium and of this communication

Normal and anomalous diffusion in evolving domains: a brief overview of some recent results

F. Le Vot[1] , **E. Abad**[2,*], C. Escudero[3], S. B. Yuste[4]

[1] *Department of Physics, University of Extremadura, Badajoz, Spain.*
[2] *Department of Applied Physics & ICCAEx, University of Extremadura, Mérida, Spain.*
[3] *Department of Fundamental Mathematics, UNED, Madrid, Spain.*
[4] *Department of Physics & ICCAEx, University of Extremadura, Badajoz, Spain.*
*e-mail: eabad@unex.es

Diffusion is usually assumed to occur in a static domain; however, evolving domains are an important paradigm in many situations of interest, as particles can actually be advected by such domains on time scales not much longer than those characteristic of diffusion. In developmental biology, say, the formation of biological structures (e.g. pigmentation or dentition patterns) happens during tissue growth [1]. Another example is the diffusion of cosmic rays in the expanding universe [2].

We will give an overview of some recent results for diffusion in deterministically growing/contracting domains. We will hereby assume that the diffusing particles stick rigidly to the evolving domain and therefore experience a drag as they wait to jump. The jump statistics of these random walkers will be taken to be independent of the parameters governing the domain's evolution.

In the case where the domain growth is controlled by a power-law scale factor, one observes a crossover between a diffusion-controlled regime and another regime where the particles' drift due to the domain evolution becomes the dominant transport mechanism [3]. In this latter scenario, diffusional mixing is strongly hindered, and a strong memory of the initial condition is retained.

Another striking effect takes place in the case of contracting domains. An exponential contraction is able to fully counterbalance diffusive spreading, resulting in the onset of a stationary positional probability density function (pdf). However, as soon as the normal diffusive process is replaced by a subdiffusive Continuous Time Random Walk, strong localization takes place, and the pdf tends to a delta function in the long-time limit (we call this effect the "Big Crunch") [4].

Finally, the effect of the domain evolution has also drastic consequences for first-passage processes and encounter-controlled reactions. These are well illustrated by several examples [5, 6], e.g., the escape of a Brownian walker from a growing hypersphere, "the target problem" in an expanding space, and the kinetics of the $1D$ encounter-controlled coalescence reaction $A + A \to A$, where A denotes a diffusing reactant. In the latter example, the chemical reactions are known to induce self-ordering in a static domain, in the sense that the reactions build up spatial correlations between a set of diffusing particles that are initially scattered at random on the real line. However, such self-ordering processes are strongly slowed down and prematurely brought to an end when the embedding domain expands at a sufficiently fast rate. In addition, a finite number of particles may survive for arbitrarily long times, and the fraction of surviving particles depends on the details of the initial condition. The obtained results highlight the need to extend the existing first-passage theories of chemical kinetics to deal with the interplay between diffusional mixing and advection induced by the evolving domain.

[1] J. D. Murray, *Mathematical Biology. II Spatial Models and Biomedical Applications*, Springer (2003).

[2] V. Berezinsky and A. Z. Gazizov, *Diffusion of Cosmic Rays in the Expanding Universe. I*, The Astrophysical Journal **643**, 8 (2006).

[3] S. B. Yuste, E. Abad and C. Escudero, *Diffusion in an expanding medium: Fokker-Planck equation, Green's function, and first-passage properties*, Phys. Rev. E **94**, 032118 (2016).

[4] F. Le Vot, E. Abad and B. Yuste, Continuous-time random-walk model for anomalous diffusion in expanding media, Phys. Rev. E **96**, 032117 (2017).

[5] F. Le Vot, C. Escudero, E. Abad and S. B. Yuste, *Encounter-controlled coalescence and annihilation on a one-dimensional growing domain*, Phys. Rev. E **98**, 032137 (2018).

[6] E. Abad, C. Escudero, F. Le Vot and S. B. Yuste, *First-Passage Processes and Encounter-Controlled Reactions in Growing Domains, in Chemical Kinetics: Beyond the Textbook*, edited by K. Lindenberg, R. Metzler and G. Oshanin, World Scientific (2019).

Acknowledgements: We acknowledge funding from the Government of Spain through Project No. FIS2016-76359-P and from the regional Extremadura Government through Projects No. GR18079 and No. IB16087, both partially funded by the ERDF.

The turning point and end of an expanding epidemic cannot be precisely forecast

Mario Castro[1,2,*], Saúl Ares[1,3], José A. Cuesta[1,4,5], and Susanna Manrubia[1,3]

[1] *Grupo Interdisciplinar de Sistemas Complejos (GISC), Madrid, Spain*
[2] *Universidad Pontificia Comillas, Madrid, Spain*
[4] *Dept. Biología de Sistemas, Centro Nacional de Biotecnología (CSIC). c/ Darwin 3, 28049 Madrid, Spain*
[4] *Dept. Matemáticas, Universidad Carlos III de Madrid, Leganes, Spain*
[5] *UC3M-Santander Big Data Institute (IBiDat), c/ Madrid 135, 28903 Getafe, Spain*
*e-mail: marioc@comillas.edu

Can the turning point and end of an expanding epidemic be precisely forecasted while the epidemic is still spreading? Epidemic spread is characterized by exponentially growing dynamics, which are intrinsically unpredictable. The time at which the growth in the number of infected individuals halts and starts decreasing cannot be calculated with certainty before the turning point is actually attained; neither can the end of the epidemic after the turning point.

An SIR model with confinement (SCIR) illustrates how lockdown measures inhibit infection spread only above a threshold that we calculate. The existence of that threshold has major effects on predictability: A Bayesian fit to the COVID-19 pandemic in Spain shows that a slow-down in the number of newly infected individuals during the expansion phase allows inferring neither the precise position of the maximum nor whether the measures taken will bring the propagation to the inhibition regime. There is a short horizon for reliable prediction, followed by a dispersion of the possible trajectories that grow extremely fast. The impossibility to predict in the midterm is not due to wrong or incomplete data, since it persists in error-free, synthetically produced data sets, and does not necessarily improve by using larger data sets.

Our study [1] warns against precise forecasts of the evolution of epidemics based on mean-field, effective or phenomenological models, and supports that only probabilities of different outcomes can be confidently given.

Also, we suggest that the future of ongoing epidemics is so sensitive to parameter values that predictions are only meaningful within a narrow time window and in probabilistic terms, much as what we are used to in weather forecasts.

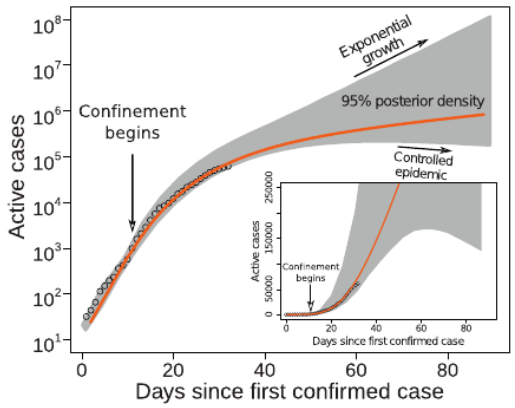

Figure 1. Fit to data obtained in real time for the daily number of active cases in Spain (from March 1st to March 29th) and peak forecast. Despite the reasonable agreement between model and empirical observations in the growing phase, opposite predictions for the future number of active cases can be derived. The solid line represents the expression for I(t) using the median parameters for the posterior distribution.

[1] Castro, M., Ares, S., Cuesta, J. A., and Manrubia, S. (2020). The turning point and end of an expanding epidemic cannot be precisely forecast. *Proceedings of the National Academy of Sciences*, 117(42), 26190-26196.

Contagion effect in exams

José Javier Arenas[1], **Pedro Carpena**[1,2,*]

[1] *Departamento de Física Aplicada II, Universidad de Málaga, Spain.* [2] *Instituto Carlos I de Física Teórica y Computacional, Universidad de Málaga, Spain.*

*e-mail: pjcarpena@uma.es

In the last decades the study of collective phenomena has produced a great interest in the field of Statistical Physics within the framework of Complex Systems, being a paradigmatic example flocking, the collective motion of self-propelled organisms [1]. More recently, these studies have been extended to collective human behavior, leading to the field of Sociophysics, in which the collective behavior emerges from the interactions of individuals as elementary units in social structures [2]. In this work we want to introduce a new example of human interaction: the possible existence of a 'social field' in a classroom where a group of students take an exam. We conjecture that the existence of social interactions could lead to a contagion effect among the students, so that a given student who delivers the exam may influence another close student to do the same, and as a result the exams are not spatially delivered at random. Our analysis is carried out by using experimental data registered in 10 high-school classrooms [3], where the students were seated randomly in isolated tables and took an exam (of different subjects). We registered both the spatial location and the exam delivery time for each student in all classrooms. We use the distances between students who finish the exam consecutively (in units of the distance between nearest neighbors) and compare these distances with the random expectation in the corresponding classroom using Monte Carlo simulations. We observe that the experimental distances are significantly (p-value $\sim 10^{-3}$) below the random expectation. This result supports the existence of a short-range spatial interaction between consecutive students (contagion effect). Based on this idea, we propose [3] a distance-driven probabilistic contagion model which works as follows: in a classroom with N students, after j students have delivered their exams and left the classroom, the last one to do so is s_j. This student may influence one of the m students remaining in the classroom located closer to s_j than $d_{\max}$, and does not affect the rest $N-j-m$ students, located further than $d_{\max}$. In this way, the probabilities of being the next one to deliver the exam for one of the affected and one of the not-affected students can be written as:

$$\mathrm{P}_m = \begin{cases} \frac{p}{m} + \frac{1-p}{N-j} & (m \neq 0) \\ 0 & (m = 0) \end{cases}, \quad \mathrm{P}_{N-j-m} = \begin{cases} \frac{1-p}{N-j} & (m \neq 0) \\ \frac{1}{N-j} & (m = 0) \end{cases}$$

Therefore, p quantifies the excess probability shared by the m close students with respect to the random expectation.

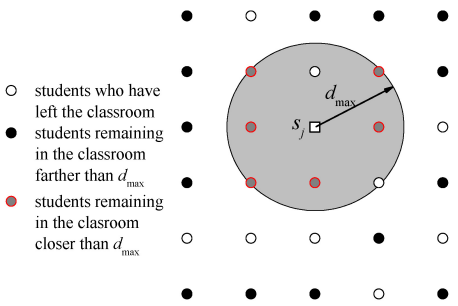

Figure 1. Schematic plot of the contagion model in a classroom with 30 students. The j-th student who delivers the exam, s_j (□) may influence students remaining in the classroom closer than $d_{\max}$ (gray circles).

The model has two input parameters: the contagion probability p and the maximum distance $d_{\max}$ at which the contagion acts (Fig. 1). We can estimate $d_{\max}$ *a priori* by observing which individual distances are clearly over represented in the experimental record as compared to the random expectation, which suggests to use $d_{\max} = 1$ as an appropriate input value. This choice leaves p as the only parameter to be determined. By running the model a large number of times with Monte Carlo simulations and comparing the corresponding results with the experimental data, we obtain a contagion probability $p \simeq 1/6$.

This spatial contagion effect could also appear in other social human activities where the interaction between subjects occurs via single events (similar to an exam delivery), such as for example raised hand votation procedures in assemblies.

[1] J. R. Usherwood, M. Stavrou, J. C. Lowe. K. Roskilly and A. M. Wilson. *Nature* **474**, 494 (2011).
[2] C. Castellano, S. Fortunato, and V. Loreto. *Rev. Mod. Phys.* **81**, 591 (2009).
[3] J. J. Arenas and P. Carpena. Submitted (2022).

Building continuous time crystals from rare events

R. Hurtado-Guiérrez[1,2], F. Carollo[3], C. Pérez-Espigares[1,2], **P.I. Hurtado**[1,2,*]

[1] *Departamento de Electromagnetismo y Física de la Materia, Universidad de Granada, Granada 18071, Spain.* [2] *Institute Carlos I for Theoretical and Computational Physics, Universidad de Granada, Granada 18071, Spain.* [3] *Institut für Theoretische Physik, Universität Tübingen, Auf der Morgenstelle 14, 72076 Tübingen, Germany.*

*e-mail: phurtado@onsager.ugr.es

Symmetry-breaking dynamical phase transitions (DPTs) abound in the fluctuations of nonequilibrium systems. Here we show that the spectral features of a particular class of DPTs exhibit the fingerprints of the recently discovered time-crystal phase of matter. Using Doob's transform as a tool, we provide a mechanism to build classical time-crystal generators from the rare event statistics of some driven diffusive systems. An analysis of the Doob's smart field in terms of the order parameter of the transition then leads to the time-crystal lattice gas (tcLG), a model of driven fluid subject to an external *packing field* which presents a clear-cut steady-state phase transition to a time-crystalline phase characterized by a matter density wave which breaks continuous time-translation symmetry and displays rigidity and long-range spatio-temporal order, as required for a time crystal. A hydrodynamic analysis of the tcLG transition uncovers striking similarities, but also key differences, with the Kuramoto synchronization transition. Possible experimental realizations of the tcLG in colloidal fluids are also discussed.

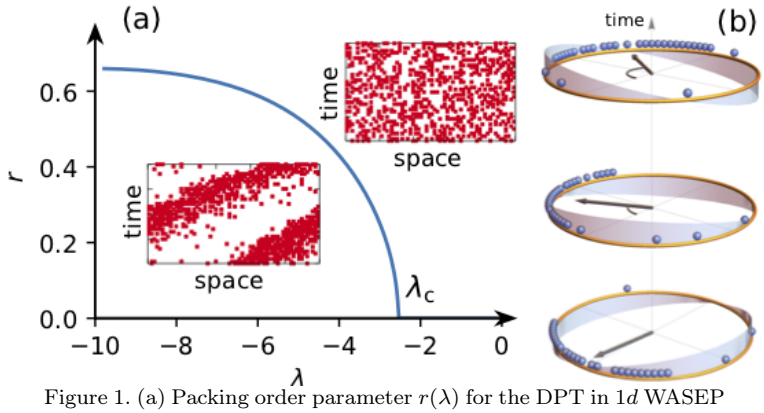

Figure 1. (a) Packing order parameter $r(\lambda)$ for the DPT in $1d$ WASEP as a function of the biasing field λ. Inset: spacetime trajectories for current fluctuations above (top) and below (bottom) the critical point. Note the density wave in the latter case. (b) Time-crystal lattice gas with a packing field (shaded curve) which pushes particles lagging behind the center of mass while restraining those moving ahead, a mechanism that leads to a a rotating condensate. The arrow locates the condensate center of mass, with a magnitude $\propto r_C$.

[1] R. Hurtado-Gutiérrez, F. Carollo, C. Pérez-Espigares and P.I. Hurtado, *Phys. Rev. Lett.* **125**, 160601 (2020).

Two lines of space reserved to include
codes of the symposium and of this communication

Multipolarity in a Complex Society

J. Borondo[1,2], R. Caballero[3], J. P. Cárdenas[4], **J. C. Losada**[1,*], G. Olivares[2], J. M. Robles[3]

[1]*Complex System Group, Universidad Politécnica de Madrid. Ciudad Universitaria s/n, Madrid, Spain.*
[2]*ICADE. Dpto. Gestión Empresarial. Universidad Pontificia de Comillas. Alberto Aguilera 23, Madrid. Spain.*
[3]*Data Science and Soft Computing for Social Analytics and Decision Aid. Univ. Complutense de Madrid. Madrid, Spain.*
[4]*Net-Works, Angamos 451, Reñaca, Viña del Mar, Chile.*

*e-mail: juancarlos.losada@upm.es

In today's hyperconnected society, online social networks have become a fundamental tool in public debate. They allow a greater participation of the citizens in the conversations and a better diffusion of their opinions, feelings or affinities. In many cases, the confrontation of ideas occurs in a socially polarized and fragmented way. Online social networks only amplify and increase this polarization, particularly in political contexts. We focus in two types of polarization:

- *Ideological polarization*, in which individuals position themselves around opposing poles of opinion represented by opinion leaders (fundamentally political leaders or parties)
- *Affective polarization*, in which users' opinions are determined by positive sentiments (love) or negative sentiments (hate) towards candidates or parties.

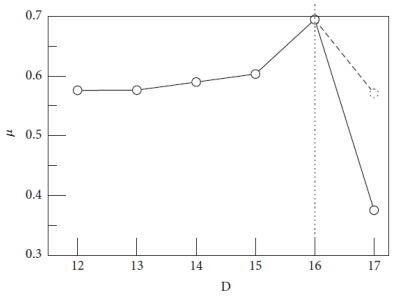

Figure 1. Evolution of the polarization index, μ, since December 11th until December 17th (day of 2017 Chilean Presidential elections). In dotted line, the values corresponding to the electoral campaign period without taking into account the users who only participated on the voting day [3].

In this work we characterize and quantify political polarization and affective polarization, analyzing the different mechanisms of interaction between Twitter users. One can define Twitter as a multilayer social network where each layer represents one of the three interaction mechanisms: following, mentioning, and retweeting. In the mentions layer, users are mainly grouped around politicians, while in the retweets layer, information is spread around the media and other opinion leaders [1]. For this reason, the layer of mentions is the appropriate one to study affective polarization, while ideological polarization is better manifested through the retweets layer.

To analyze the ideological polarization, we infer a continuous opinion distribution by applying a model based on retweet interactions, previously detecting elite users with fixed and antagonist opinions, labeled as +1 and -1 [2].

To analyze the affective polarization, we apply sentiment analysis techniques to the messages mentioning the candidates. Thus, we assign a numerical value to the sentiment of the users towards each candidate, where -1 implies extreme hate, +1 extreme love and 0 indifference [3]. From the distributions of opinions/sentiments, p(x), we compute the polarization index initially described in ref [4]: $\mu = (1 - |\Delta A|)d$, where $|\Delta A|$ is the difference between users in each interval $x < 0$ and $x > 0$, and d is half the distance between the gravity centers of the two groups of opinions.

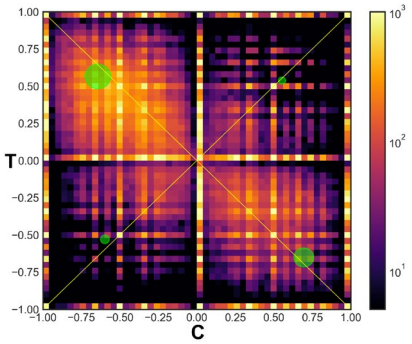

Figure 2. Love-Hate diagram for candidates T and C. The gravity center of each quadrant is shown as green circles with diameters proportional to the number of users in the quadrant [4].

Fig. 1 shows the temporal evolution of the ideological polarization index in the presidential elections in Chile 2017 [2]. Fig 2 shows the love/hate diagram obtained by analyzing affective polarization in the 2016 USA elections towards H. Clinton and D. Trump [3].

[1] J. Borondo, A.J. Morales, R.M. Benito, J.C. Losada. Multiple leaders on a multilayer social media, *Chaos, Solitons & Fractals* **72**, 90 (2015).
[2] G. Olivares, J. P. Cárdenas, J. C. Losada, J. Borondo. Opinion Polarization during a Dichotomous Electoral Process. *Complexity* **2019**, 5854037 (2019)
[3] Losada, J.C., Robles, J.M., Benito, R.M., Caballero, R. Love and Hate During Political Campaigns in Social Networks. *Complex Networks & Their Applications X,* 66-77. Springer, Cham. (2022).
[4] A. J. Morales, J. Borondo, J. C. Losada, and R. M. Benito. Measuring political polarization: Twitter shows the two sides of Venezuela, *Chaos: An Interdisciplinary Journal of Nonlinear Science* **25**, 033114 (2015).

Two lines of space reserved to include
codes of the symposium and of this communication

Evolutionary Dynamics of The Ethereum Transaction Network

M Grande[3,5,*], F Borondo[1,2], J Borondo[4,5]

[1]*Instituto de Ciencias Matematicas (ICMAT); Campus de Cantoblanco UAM; Nicolas Cabrera, 13-15; 28049 Madrid (Spain).* [2]*Departamento de Quimica; Universidad Autonoma de Madrid; CANTOBLANCO - 28049 Madrid (Spain).*[3]*Grupo de Sistemas Complejos; Universidad Politecnica de Madrid; 28035 Madrid (Spain).*[4]*Departamento de Gestion Empresarial; Universidad Pontificia de comillas ICADE; Alberto Aguilera 23; 28015 Madrid (Spain).*[5]*AGrowingData; Navarro Rodrigo 2 AT; 04001 Almeria (Spain).*

*e-mail: margrande45@gmail.com

We are witnessing a revolution in the financial system, which is being replaced by the new and innovative Decentralized Finance (DeFi). DeFi projects are tackling long-standing problems and addressing inefficiencies in our current system, improving financial inclusion, increasing liquidity and reducing costs. Unlike the traditional system, where financial applications are difficult to access, rigid, hard to use and expensive, DeFi applications are open and permisionless. Anyone can access them, all they need is an internet connection.

But what really makes this self-organized market of digital currencies attractive for the research community is that all transactions are publicly available, in contrast to the traditional financial system. This represents an unprecedented scenario that allows us to understand and explain the evolution and adoption of a financial system by capturing the complex behavior that emerges from the relationships between users.

In this work we focus on the Ethereum Blockchain, the largest decentralized computing platform in terms of users and usage. We have analyzed the transactions that occur in the network under a complex system perspective, in which nodes are the accounts that operate and links represent the transactions between them. We describe the dynamics and evolution of the system by analyzing its structure and computing its properties over time. Finally, we explore the relationships that exist between these properties and the future price of the network cryptocurrency called Ether (ETH).

Since this system is an evolving system, it is important to define dynamic intervals that capture the evolution of the system. Unlike other works that propose to create networks with an arbitrary time interval, [2], we use the method developed by Darst et al. in [1], that detects evolutionary changes in the configuration of a complex system and generates intervals accordingly. In this method, the size of each interval is determined by maximizing the similarity between the sets of events within consecutive intervals.

We applied the Dynamic time-slicing method [3] on our dataset and found that the activity of the network can be measured by considering regular time intervals of 14 days. We also found a strong correlation between the similarity score obtained from the Dynamic time-slicing method and the Ethereum price.

Next, we analyzed the properties of the resulting networks and found that the degree distribution of the networks are highly heterogeneous, where a small fraction of addresses tend to trade with the vast majority, while most addresses hardly trade with others. We found that the networks are disassortative and present very low clustering.

Finally, we explored the relations between the network properties and the future price of Ethereum and found a strong negative correlation between the exponent of the degree distribution and the price. Hence, our results suggest that the transaction network contains relevant information to explain the evolution and adoption of the system.

[1] A. Darst, R. K., B. Granell, C., C. Arenas, A., D. Gomez, S., E Saramaki, J., and F Fortunato, S., *Detection of timescales in evolving complex systems. Scientific reports* **6**, 39713 (2016).

[2] A. Liang, J., B. Li, L., and C. Zeng, D. *Evolutionary dynamics of cryptocurrency transaction networks: An empirical study. PloS one*, **13(8)** (2018).

[3] `https://github.com/rkdarst/dynsnap/blob/master/doc/Manual.rst`

Numerical sampling rare of rare trajectories using stochastic bridges

Raul Toral

IFISC (Instituto de Física Interdisciplinar y Sistemas Complejos), Universitat de les Illes Balears-CSIC, Palma de Mallorca

*e-mail: raul@ifisc.uib-csic.es

In stochastic systems the most uncommonly occurring events are often the ones that are most consequential. Typical examples beyond the escape of a Brownian particle in a double-well potential include the dynamics of biological switches, the extinction of species in ecology and large fluctuations in chemical reactions. We have recently introduced a numerical method to draw the ensemble of stochastic trajectories that link together any two points (or regions) in phase space [1]. For a given target stochastic process, we construct a stochastic bridge linking initial and final points by defining a new stochastic dynamics that runs reversed in time. This is combined with a recent method to sample events with a very low probability using weighted-ensemble techniques. We show that the statistics of the target process can be recovered by associating a statistical weight with each stochastic bridge. This allows us to dedicate more computational effort to rare trajectories without introducing bias or interdependence. The method is flexible; the target process is fully general, detailed balance is not required, no small-noise approximation is made, and it is not limited to the sampling of trajectories associated to a target macroscopic quantity, nor does it require the introduction of artificial parameters such as temperatures.

We show through several examples that the possibility of sampling the ensemble of trajectories unveils the whole statistical picture of these unlikely-yet-important events, in contrast to the Wentzel-Kramers-Brillouin (WKB) optimal paths, which we verify are only relevant in the limit of small noise. We are able to show that the stochastic bridges produced this way provide the full statistics of the ensemble of transition paths between long-lived states of the target process. This allows one to sample fluctuations around the WKB instanton, and thus to judge if the WKB approximation scheme is accurate at various levels of noise. As an example we show in the figure several (rare) extinction trajectories of an Susceptible-Infected-Susceptible model in the endemic regim and compare them with the predictions of the WKB theory valid in the limit of a large population. Other examples we will analyze in this presentation include the distribution of first-passage times of a biased random walk and the generation of noise-driven transitions from the undifferentiated to either one of the differentiated cell states in a model of cell differentiation.

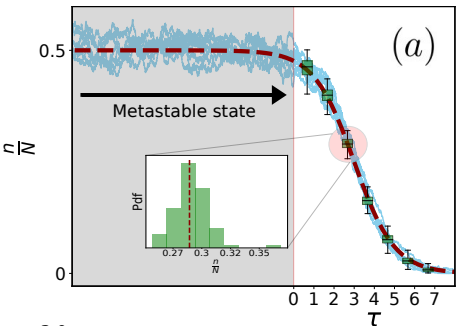

Figure 1. Extinction trajectories for the SIS model compared to the WKB instanton. n is the number of infected individuals in a population of total size N. The inset shows the pdf of n at the given time.

[1] J. Aguilar, J. W. Baron. T. Galla, R. Toral, *arXiv:2112.08252*.

Acknowledgements: Partial financial support has been received from the Agencia Estatal de Investigación (AEI, MCI, Spain) and Fondo Europeo de Desarrollo Regional (FEDER, UE) under Project PACSS (RTI2018-093732-B-C21/C22), and the María de Maeztu Program for units of Excellence in R&D, grant MDM-2017-0711 funded by MCIN/AEI/10.13039/501100011033.

Optimal control of bidirectional escape from a symmetric potential well

R. Chacón[1,2], P. J. Martínez[3],**J. M. Marcos**[4,*], F. J. Aranda[5], J. A. Martínez[6]

[1] *Departamento de Física Aplicada, Escuela de Ingenierías Industriales, Universidad de Extremadura, Apartado Postal 382, E-06006 Badajoz, Spain* [2] *Instituto de Computación Científica Avanzada (ICCAEx), Universidad de Extremadura, E-06006 Badajoz, Spain* [3] *Departamento de Física Aplicada, E.I.N.A., Universidad de Zaragoza, E-50018 Zaragoza, Spain and Instituto de Nanociencia y Materiales de Aragón (INMA), CSIC-Universidad de Zaragoza, E-50009 Zaragoza, Spain* [4] *Departamento de Física, Facultad de Ciencias, Universidad de Extremadura, E-06006 Badajoz, Spain* [5] *Departamento de Ingeniería Eléctrica, Electrónica y Automática, Facultad de Ciencias, Universidad de Extremadura, E-06006 Badajoz, Spain* [6] *Departamento de Ingeniería Eléctrica, Electrónica y Automática, Escuela de Ingenieros Industriales, Universidad de Castilla-La Mancha, E-02071 Albacete, Spain*

*e-mail: jesusmm@unex.es

We have investigated the effectiveness of zero average periodic forces at yielding directed ratchet escape from a symmetric potential well by considering an asymmetric external periodic force. Optimal enhancement of directed ratchet escape is predicted to occur when the wave form of the zero-average periodic force acting on a damped driven oscillator matches as closely as possible to a biharmonic universal wave form, as predicted by the theory of ratchet universality. Our numerical experiments confirmed those findings, as well as revealed the interplay between heteroclinic instabilities leading to chaotic escape and breaking of a generalized parity symmetry leading to directed ratchet escape to an attractor either at ∞ or at $-\infty$. Specifically, the optimal approximation to the biharmonic universal force triggers the almost complete destruction of the nonescaping basin for driving amplitudes which are systematically lower than those corresponding to a symmetric periodic force having the same period.

[1] R. Chacón, P. J. Martínez, J. M. Marcos, F. J. Aranda and J. A. Martínez, *Phys. Rev. E* **103**, 022203 (2021).

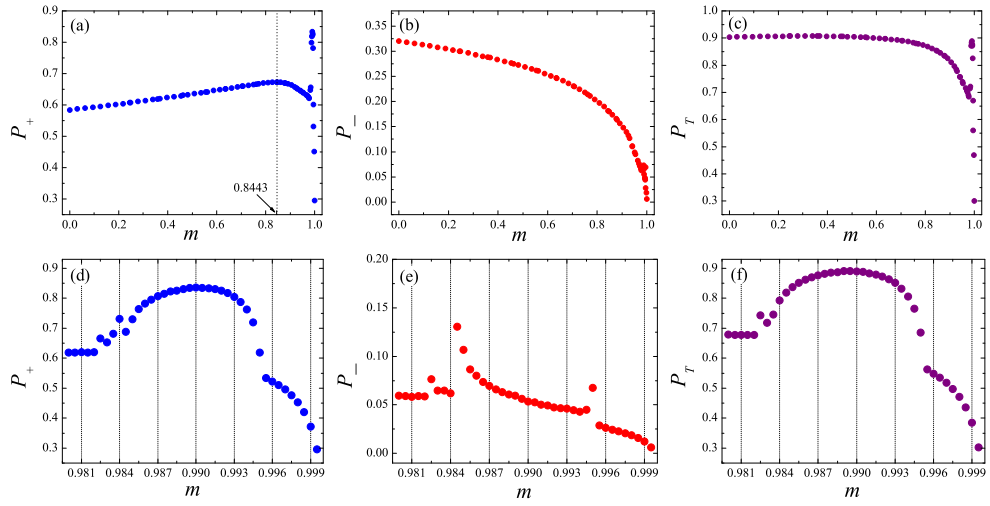

Figure 1. Escape probabilities P_+ (a), P_- (b), $P_T = P_+ + P_-$ (c) of the one-well Duffing oscillator $(\ddot{x} + x - 4x^3 = -\delta\dot{x} + \gamma F(t))$ subjected to the elliptic force $F_{ellip}(t; T, m) \equiv sn(\Omega t; m)cn(\Omega t; m)$ vs the shape parameter m. Versions (d), (e), and (f) show enlargements of the versions (a), (b), and (c) over the range $0.98 < m < 1$, respectively. System parameters: $\delta = 0.2$, $\gamma = 0.28$, $T = 2/0.5268$. The quantities plotted are dimensionless.

Colloidal monolayers: bridging the gap between two and three spatial dimensions

Alvaro Domínguez

Departamento de Física Atómica, Molecular y Nuclear, Universidad de Sevilla, Apdo. 1065, 41080 Spain.

*e-mail: dominguez@us.es

It is well established that, unlike for a three-dimensional fluid, particle interactions prevent the hydrodynamic transport coefficients from being defined for a two-dimensional fluid due to the notorious "long-time tail" feature of the velocity autocorrelation.

A colloidal monolayer formed at a fluid interface builds a bridge between these two limiting cases, and it provides insight on the transition from three down to two spatial dimensions: the positions of the colloidal particles are constrained to a plane and the colloid thus resembles a two-dimensional fluid. But the exchange of particle momentum takes place in three-dimensional space because it is mediated by the ambient fluid in the form of hydrodynamic interactions.

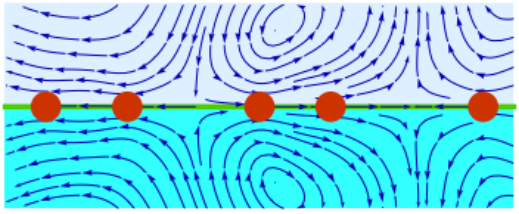

Side view of a colloidal monolayer formed at the interface between two fluids, and sketch of the three-dimensional flows responsible for the hydrodynamic interactions.

Here we study the behavior of the colloidal diffusivity, which is the only hydrodynamic transport coefficient for the two-dimensional colloidal fluid. The starting point is the Smoluchowski equation, i.e., the Fokker-Planck equation for the colloidal particles in the overdamped regime with due account of the hydrodynamic interactions. We then show that the diffusivity exhibits an intermediate behavior between purely two-dimensional and fully three-dimensional fluid: on the one hand, Fick's law, which pertains to *collective diffusion*, breaks down altogether [1-3], as confirmed experimentally [4]. On the other hand, the coefficient of *self-diffusion* (or single–particle diffusion) is finite [5], but the transitional nature of the monolayer shows up in a non-analytic dependence on the colloidal packing fraction [6], at odds with the case of a fully three-dimensional colloid.

[1] J. Bleibel, A. Domínguez, F. Günther, J. Harting, M. Oettel, *Soft Matter*, **10**, 2945 (2014).
[2] S. Panzuela, R. P. Peláez, R. Delgado-Buscalioni, *Physical Review E*, **95**, 012602 (2017).
[3] J. Bleibel, A. Domínguez, M. Oettel, *Physical Review E*, **95**, 032604 (2017).
[4] B. Lin, B. Cui, X. Xu, R. Zangi, H. Diamant, S. A. Rice, *Physical Review E*, **89**, 022303, (2014).
[5] R. P. Peláez, F. Balboa Usabiaga, S. Panzuela, Q. Xiao, R. Delgado-Buscalioni, A. Donev, *Journal of Statistical Mechanics: Theory and Experiment*, 063207 (2018).
[6] A. Domínguez, unpublished (2022).

Two lines of space reserved to include
codes of the symposium and of this communication

Kinetic theory of fluids under strong confinement

P. Maynar[1,2,*], M. I. García de Soria[1,2], J. J. Brey[1,2]

[1] *Área de Física Teórica, Universidad de Sevilla, Spain.* [2] *Institute for Theoretical and Computational Physics, Universidad de Granada, Spain.*

*e-mail: maynar@us.es

A kinetic equation for a system of elastic hard spheres or disks confined by a hard wall of arbitrary shape is derived. It is a generalization of the modified Enskog equation in which the effects of the confinement are taken into account and it is supposed to be valid up to moderate densities. A Lyapunov functional, $\mathcal{H}[f]$, is identified. For any solution of the kinetic equation, $\mathcal{H}$ decays monotonically in time until the system reaches the inhomogeneous equilibrium distribution, that is a Maxwellian distribution with a the density field consistent with equilibrium statistical mechanics. From the equation, balance equations for the hydrodynamic fields are derived, identifying the collisional transfer contributions to the pressure tensor and heat flux. This let us to formulate a generalization of the wall theorem to arbitrary non-equilibrium states [1]. The results are generalized to inelastic hard spheres and the extreme case in which the system is confined by two hard walls separated a distance smaller than twice the diameter of the particles is studied in detail [2].

[1] P. Maynar, M. I. García de Soria, and J. J. Brey, *J. Stat. Phys.* **170**, 999 (2018).
[2] P. Maynar, M. I. García de Soria, and J. J. Brey, *Phys. Rev. E* **99**, 032903 (2019).

Optimal thermalisation for a generic d-dimensional harmonic oscillator

Antonio Patrón*, Antonio Prados, and Carlos A. Plata

Física Teórica, Universidad de Sevilla, Apartado de Correos 1065, E-41080 Sevilla, Spain

*e-mail: apatron@us.es

In this work, we study the optimisation problem of minimising the connection time between equilibrium states for an overdamped Brownian particle confined in a d-dimensional harmonic trap, in which the temperature is externally controlled. This system constitutes a paradigmatic model of theoretical interest within the field of stochastic thermodynamics. Moreover, it is also relevant in the experimental context, for it allows to describe accurately the dynamics of realistic systems such as confined colloidal particles in optical traps. The state of the system is fully determined via the variances $z_i \equiv \langle x_i^2 \rangle$, $i = 1, ..., d$, with x_i being the i-th spatial component of the particle. Their time evolution is given via the dynamic equations

$$\frac{dz_i}{dt} = -2k_i z_i + 2T(t), \quad i = 1, ..., d, \tag{1}$$

with k_i being the elastic constant of the harmonic trap in the i-th direction, and $T(t) \in [T_{\min}, T_{\max}]$ being the bath temperature, which is externally controlled at will.

The optimal functional form of $T(t)$ that minimises the connection time between two equilibrium states of the system is sought. Such states are characterised by the initial and final temperatures T_0 and T_f, respectively. Direct application of control theory, specifically Pontryagin's maximum principle, shows that optimal protocols for the temperature are of the *bang-bang* type, that is, the protocol comprises several time windows in which the temperature must take alternatively the minimum ($T_{\min}$) and maximum ($T_{\max}$) values allowed.

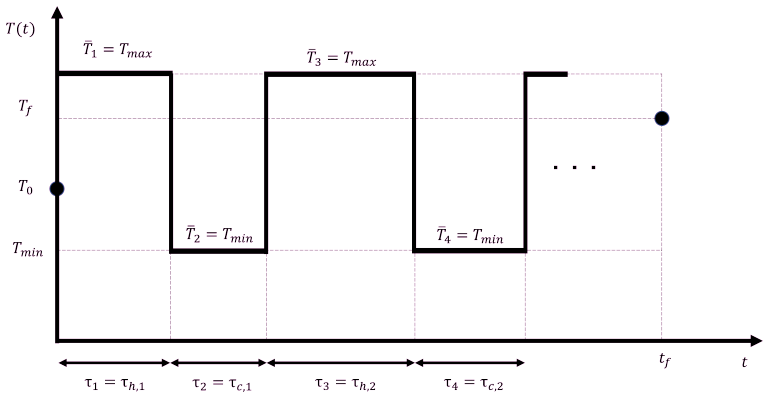

Figure 1. Sketch of the optimal bang-bang control able to connect two equilibrium states of a d-dimensional harmonic oscillator.

For the system of concern, we show that it is possible to explicitly work out the optimal thermal connections. We study their dependence on the limiting values of the temperature, and also on the elastic constants k_i that characterise the confinement in each direction. A rich phenomenology emerges, including striking discontinuities on the minimum connection times when two or more of the elastic constants become equal.

[1] Antonio Patrón, Antonio Prados, and Carlos A. Plata, unpublished
[2] Carlos A. Plata, David Guéry-Odelin, E. Trizac, and A. Prados, Phys. Rev. E 99, 012140 (2019)
[3] Martínez I A, Roldán E, Dinis L, Petrov D and Rica R A 2015 Physical Review Letters 114 120601

Acknowledgements: Support from Grant PGC2018-093998-B-I00 funded by MCIN/AEI/10.13039/501100011033/ and by ERDF "A way of making Europe." is acknowledged. C.A.P. acknowledges financial support from Junta de Andalucía and European Social Fund through the program PAIDI-DOCTOR. A. Patrón acknowledges support from the FPU programme through Grant FPU2019-4110.

Direct evaluation of large deviations in open quantum systems

F. Carollo[3], C. Pérez-Espigares[1,2,*]

[1]*Departamento de Electromagnetismo y Física de la Materia, Universidad de Granada, Granada 18071, Spain.*
[2]*Institute Carlos I for Theoretical and Computational Physics, Universidad de Granada, Granada 18071, Spain.*
[3]*Institut für Theoretische Physik, Universität Tübingen, Auf der Morgenstelle 14, 72076 Tübingen, Germany.*

*e-mail: carlosperez@ugr.es

Controlling dynamical fluctuations in open quantum systems is essential both for our comprehension of quantum nonequilibrium behavior and for its possible application in near-term quantum technologies. However, understanding these fluctuations is extremely challenging due, to a large extent, to a lack of efficient important sampling methods for quantum systems. In this talk, we present a unified framework—based on population-dynamics methods—for the evaluation of the full probability distribution of generic time-integrated observables in Markovian quantum jump processes. These include quantities carrying information about genuine quantum features, such as quantum superposition or entanglement, not accessible with existing numerical techniques. The algorithm we propose provides dynamical free-energy and entropy functionals which, akin to their equilibrium counterpart, permit one to unveil intriguing phase-transition behavior in quantum trajectories.

[1] F. Carollo and C. Pérez-Espigares, *Physical Review E* **102**, 030104(R) (2020).

Two lines of space reserved to include
codes of the symposium and of this communication

Nonlinearity test for complex time series

A. V. Coronado[1], P. A. Bernaola-galván[1,2], M. Gómez-Extremera[1] and P. Carpena[1,2,*]

[1] *Departamento de Física Aplicada II, Universidad de Málaga, Spain.* [2] *Instituto Carlos I de Física Teórica y Computacional, Universidad de Málaga, Spain.*

*e-mail: pjcarpena@uma.es

The nonlinear character of a dynamical system can be studied from the corresponding dynamical equations. Note that the knowledge of the dynamics is essential for both understanding properly the analyzed system and for modeling purposes. However, in the majority of the complex systems of interest, such dynamical equations are not known, and the only available information from the system is typically an output observable time series. Thus, the possible underlying nonlinear dynamics must be assessed from the available time series by applying nonlinearity tests on these data, able to determine if the analyzed time series exhibits or not nonlinear properties.

The canonical reference for linear stochastic time series are stochastic Gaussian time series with only linear correlations. However, the available experimental time series are rarely Gaussian. Therefore, the most widely used nonlinearity test [1] generates surrogate time series with the same marginal (non Gaussian) distribution, and more important, with the same autocorrelation values as the analyzed time series. This property is achieved by calculating the power spectrum of the experimental time series via FFT, and create a signal in the frequency domain with this power spectrum but applying phase randomization to destroy nonlinear correlations. Once the phase-randomized signal in the frequency domain is Fourier-transformed back into real space, a final time series is obtained with the same autocorrelation values as those of the analyzed signal according to the Wiener-Khinchin theorem, but purely linear due to the phase randomization procedure. However, this time series does not present the same marginal distribution as the experimental one, and an iterative process is required [1] to get the same correlations and distributions as the original data. A Monte Carlo set of these surrogate time series is generated, and constitutes the null hypothesis that is statistically tested against the experimental time series to determine its possible nonlinear character.

However, some studies [2] show that the iterative process in [1] needed to create surrogate data introduce correlations in the Fourier phases, therefore producing surrogate time series with nonlinear properties, which are then not adequate to be considered as the reference for linearity. Here, we present a nonlinearity test of general applicability which do not require the generation of surrogate data. Recently [3], we have shown than if a purely linear Gaussian correlated time series is transformed into another time series with different marginal distribution then the autocorrelation C of this time series can be obtained from the correlation C_G of the Gaussian time series by:

$$C = \int_{-\infty}^{\infty}\int_{-\infty}^{\infty} F^{-1}(\Phi(x_G))\, F^{-1}(\Phi(y_G))\, \varphi_2(x_G, y_G, C_G)\, \mathrm{d}x\, \mathrm{d}y$$

where x_G and y_G are Gaussian variables, $\varphi_2()$ is the bivariate Gaussian distribution, $\Phi()$ is the Gaussian cumulative distribution, and $F^{-1}()$ is the inverse cumulative distribution of the final non Gaussian times series. This equation holds if and only if the original Gaussian and the final non Gaussian time series are purely linear. Thus, we can use it to construct a nonlinearity test as follows: a) Given a time series, calculate the autocorrelation function C. b) Use this C value and solve numerically the equation to determine the autocorrelation function C_G, which corresponds to the Gaussian linear time series from where the analyzed time series would have been hypothetically obtained if and only if it is purely linear. c) Transform the analyzed time series to follow a Gaussian distribution and calculate the autocorrelation function C'_G. If the original time series is linear then (statistically) $C_G = C'_G$, but if $C_G \neq C'_G$ then we can conclude that the analyzed time series possess nonlinear character. We have applied this test to a great variety of known linear and nonlinear time series, and have obtained excellent results [4].

[1] T. Schreiber and A. Schmitz. *Phys. Rev. Lett.* **77**, 635 (1996).

[2] C. Räth, M. Gliozzi, I. E. Papadakis and W. Brinkmann. *Phys. Rev. Lett.* **109**, 144101 (2012).

[3] P. Carpena, P. Bernaola-Galván, M. Gómez-Extremera and A. V. Coronado. *Chaos* **30**, 083140 (2020).

[4] P. Carpena, P. Bernaola-Galván, M. Gómez-Extremera and A. V. Coronado (in preparation).

Statistical models of social interaction

Samuel Martin-Gutierrez[1,2,*], Juan C. Losada[1], Rosa M. Benito[1]

[1] *Grupo de Sistemas Complejos, Escuela Técnica Superior de Ingeniería Agronómica, Alimentaria y de Biosistemas, Universidad Politécnica de Madrid, Av. Puerta de Hierro, 2, 28040 Madrid, Spain.*
[2] *Network Inequality group, Complexity Science Hub Vienna, Josefstädter Str. 39, 1080, Wien, Austria*
*e-mail: martin.gutierrez@csh.ac.at

In this work [1] we present three mathematical models to explain how the actions performed by an individual (her activity) influence the collective reaction (or response) of the social system she is embedded in. The models consider different levels of dependence between response and activity. In the first model, we consider activity and response completely independent (Independent Variables model – InV), while in the second and third models individual activity influences collective response. The main difference between these last two models is the distinguishability of the actors. In the Identical Actors (IdA) model, the system is agnostic with respect to the individual that performs the actions, while in the Distinguishable Actors (DiA) model, the dependence between activity and response is determined by the features of the actor that performs the action. In Figure 1 we present a diagram that summarizes the main ideas behind each model.

We use the models to obtain the distribution of the efficiency metric η, defined as the ratio between the number of reactions R triggered by an actor on other members of the system and the number of actions A of the actor:

$$\eta = \frac{R}{A}$$

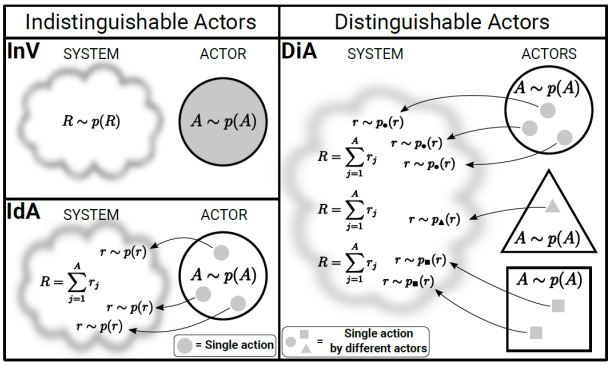

Figure 1. Diagram that summarizes the main characteristics of the three models: Independent Variables (InV), Identical Actors (IdA) and Distinguishable Actors (DiA).

This metric is a generalization of the user efficiency [2]. We tested the models on 29 datasets from three systems of different nature: Twitter conversations, where A and R are tweets and retweets, respectively; the scientific citations network, where A and R are publications and citations; and the Wikipedia collaboration environment, where A is the number of editions and R the number of received messages. In all the systems the efficiency distribution presents a universal shape, illustrated in Figure 2, with small but relevant differences between systems.

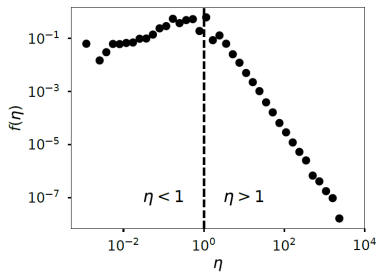

Figure 2. Empirical efficiency distribution corresponding to a Twitter conversation.

The Independent Variables model explains the universal shape of the efficiency distribution and its independence with respect to changes in the activity distribution, two fundamental characteristics for which there was previously only empirical evidence. Additionally, it reproduces the efficiency distribution for the scientific citations network. However, for Twitter and Wikipedia there are small discrepancies with the data caused by $A-R$ correlations. We incorporated these correlations in a parsimonious way in the Identical Actors model and improved the results for both systems. In particular, the IdA model reproduces adequately the right tail ($\eta > 1$) for Twitter and Wikipedia, but not the left tail ($\eta < 1$). To solve these discrepancies, we developed the Distinguishable Actors model, which fits the Twitter data remarkably well.

[1] Martin-Gutierrez, S., Losada, J.C., Benito, R.M., *Sci Rep* **10(1)**, 12126 (2020).
[2] Morales, A.J., Borondo, J., Losada, J.C., Benito, R.M., *Soc Networks* **39**, 1-11 (2014).

Acknowledgements: This work has been supported by the Spanish Ministry of Science, Innovation and Universities (MICIU) under Contract No. PGC2018-093854-B-I00, Spanish Ministry of Education, Culture and Sport (Grant No. FPU15/01461), and by the Austrian research agency (FFG) under project No. 873927.

Two lines of space reserved to include
codes of the symposium and of this communication

Dynamics of hard particles confined by an isotropic harmonic potential

M. I. García de Soria[1,2,*], P. Maynar[1,2], E. Trizac[3], and D. Guéry-Odelin[4]

[1] *Área de Física Teórica, Universidad de Sevilla, Spain.* [2] *Institute for Theoretical and Computational Physics, Universidad de Granada, Spain.* [3] *LPTMS, Université Paris-Saclay, France.* [4] *Laboratoire Collisions, Agrégats, Réactivité, Université de Toulouse, France.*

*e-mail: gsoria@us.es

The dynamics of a system composed of elastic hard particles confined by an isotropic harmonic potential is studied. In the low-density limit, the dynamics is described by the Boltzmann equation and the system does not reach equilibrium except for some particular class of initial conditions. On the contrary, the system reaches a periodic in time state in which the velocity distribution function is Gaussian, but with the hydrodynamic fields oscillating in time with some specific profiles. It is shown that this so-called *breather* state is completely specified by the constants of the motion, the mean square displacement, $\langle r^2 \rangle$, at the initial time and its derivative with respect to time also at the initial time. This is due to the fact that, at this level of description, $\langle r^2 \rangle$ verifies a closed second order differential equation. For low but finite densities, the dynamics of the system is analyzed by taking into account the finite size of the particles. Under well-controlled approximations, a closed evolution equation for $\langle r^2 \rangle$ is derived, obtaining that it decays to its equilibrium value, oscillating with a frequency slightly modified with respect to the Boltzmann values. The time average of the oscillations is also renormalized. An excellent agreement is found between Molecular Dynamics simulation results and the theoretical predictions for the frequency and the time average of the oscillations. For the relaxation time, the agreement is not as good as for the two previous quantities and the origin of the discrepancies is discussed.

Two lines of space reserved to include
codes of the symposium and of this communication

Variability of spreading rate in forced plumes

Pilar López[1], **Benjamín Skadden**[2,3*], Ania Matulka[4], Ana M. Tarquis[2,3], Juan Carlos Losada[3]

[1]*Department of Biodiversity, Ecology and Evolution, Unit, University Complutense of Madrid, 28040 Madrid, Spain.* [2]*CEIGRAM, ETSIAAB, Universidad Politécnica de Madrid, 28040 Madrid, Spain.* [3]*Grupo de Sistemas Complejos (GSC), Universidad Politécnica de Madrid, 28040 Madrid, Spain.* [4]*Department of Physical Environment Area, Puertos del Estado, 28042 Madrid, Spain*

*e-mail: benjaskat2@gmail.com

The geophysical importance of forced turbulent plumes is evident as they are a fundamental part of dispersion processes, for example, volcanic plumes. From the earliest investigations, it became clear that one fundamental problem was to determine the value of the entrainment coefficient. In Morton's initial theory, the entrainment coefficient is supposed to be constant. One way to approach the analysis of the entrainment is to study the spreading rate (β). The spreading assumption establishes that the width of a plume increases at a rate proportional to a characteristic spreading velocity. In a quiet environment, there is a simple spreading relationship in which the β represents the linear increase of the dominant eddy dimension with distance from the source. However, several studies have shown that the entrainment coefficient, and therefore β, is not constant (see [1] and references therein).

Forced plumes experiments were set up to be recorded at the height of 2cm (Ho) and two Atwoods (A) [2], using frame-sequencer software (VirtualDubMod). Each image of the sequence was binarised [3]. The recorded plume measurements in all the axial extensions were obtained based on the geometrical information. Its use in a sequence of consecutive images allows the analysis of the vertical and radial measurements' evolution in time (Fig. 1).

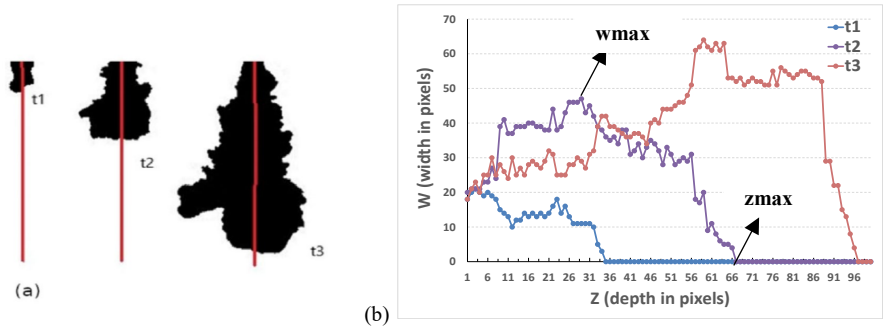

Figure 1. (a) Time development of a plume at different times (t1 = 0.02, t2 = 0.18 and t3 = 0.48 s). (b) Vertical profile of the plume width under conditions Ho = 2 cm and A= 0.01 at each time. The position of maximum width (wmax) and maximum depth (zmax) are pointed at t2.

We can define the local spreading rate, βlocal, by using the width (wi) corresponding to each depth (zi) each time and dividing it by zmax at that time (Fig. 2). When wi is wmax the value obtained is the classical spreading rate (βclassic) [2]. This methodological approach has the advantage of being non-invasive and easily exportable. Further research is in progress to analyse the dependence of the βlocal on Ho and A.

Accelerating out-of-equilibrium critical dynamics via magnetic domains

Isidoro González-Adalid Pemartín[1,*], Emanuel Mompó[2], Antonio Lasanta[3,4], Víctor Martín-Mayor[1,5], and Jesús Salas[2,4]

[1] *Departamento de Física Teórica, Universidad Complutense, 28040 Madrid, Spain.* [2] *Departamento de Matemáticas, Universidad Carlos III de Madrid, 28911 Leganés, Spain.* [3] *Departamento de Álgebra, Facultad de Educación, Economía y Tecnología de Ceuta, Universidad de Granada, Cortadura del Valle, s/n, 51001 Ceuta, Spain.* [4] *Grupo de Teorías de Campos y Física Estadística, Instituto Gregorio Millán, Universidad Carlos III de Madrid, Unidad Asociada al Instituto de Estructura de la Materia, CSIC, Spain.* [5] *Instituto de Biocomputación y Física de Sistemas Complejos (BIFI), 50018 Zaragoza, Spain.*

*e-mail: isidorog@ucm.es

Reaching thermal equilibrium fast is an important problem in science and industry. For this reason, the non-equilibrium relaxation has been very studied during the last decades. In fact, the attention received by the counterintuitive Mpemba Effect [1], allowing to cool down faster the hotter of two systems (or heat up faster the cooler system), is reasonable. Indeed, we now understand the general conditions that allow a faster cooling, or faster heating, in a variety of systems like granular matter, spin glasses, or classical and quantum Markovian systems. This knowledge allows to develop better strategies for cooling, or heating, a system. In particular, Amit and Raz have recently designed a faster heating protocol for systems with timescale separation [2].

However, a timescale separation is not present in a second-order phase transition, where critical slowing down evidences a continuum of timescale. In this situation, understanding the mechanism that governs the dynamics is the key to potentially control the evolution. The size of the ordered domains when the system enters the symmetry-broken phase is a natural candidate as a driver for this mechanism.

In our work [3], we focus on the study of the ferromagnetic two-dimensional (2D) Ising spin model. In particular, we study through numerical simulations an unexplored out-of-equilibrium heating protocol, in which the bath temperature starts below the critical temperature, in the ferromagnetic phase (FM), and is later heated above the critical point, in the paramagnetic phase (PM). We show that a faster relaxation can be reached in absence of timescale separation by manipulating the system's internal structure of ordered domains (related with the coherence length ξ) thanks to this excursion in the symmetry-broken phase, see Fig 1.

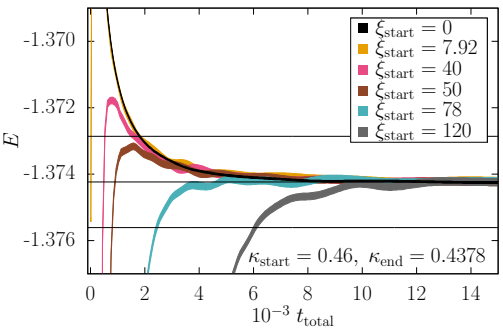

Figure 1. Energy density as a function of the total time $t_{\rm total}$ elapsed since the beginning of our protocol, as computed with the Metropolis dynamics for $\kappa_{\rm start} = 0.46$ (FM), $\kappa_{\rm end} = 0.4378$ (PM), and several values of $\xi_{\rm start}$. Values of $\xi_{\rm start}$ increase from top to bottom. The width of the curves is four times the statistical errors. The three horizontal lines correspond to $E_{\rm eq}$ multiplied by 1.001, 1 and 0.999.

[1] E. B. Mpemba and D. G. Osborne, *Phys. Educ.* **4**, 172 (1969).
[2] A. Gal and O. Raz, *Phys. Rev. Lett.*, **124**, 060602 (2020).
[3] I. González-Adalid Pemartín, E. Mompó, A. Lasanta, V. Martín-Mayor and J. Salas, *Phys. Rev. E*, **104**, 044114 (2021).

Acknowledgements: This work was partially supported by Ministerio de Economía, Industria y Competitividad (MINECO, Spain), Agencia Estatal de Investigación (AEI, Spain), and Fondo Europeo de Desarrollo Regional (FEDER, EU) through Grants No. PGC2018-094684-B-C21, No. FIS2017-84440-C2-2-P, and No. MTM2017-84446-C2-2-R. A.L. and J.S. were also partially supported by Grant No. PID2020-116567GB-C22 AEI/10.13039/501100011033. A.L. was also partly supported by Grant No A-FQM-644-UGR20 Programa operativo FEDER Andalucía 2014–2020. J.S. was also partly supported by the Madrid Government (Comunidad de Madrid-Spain) under the Multiannual Agreement with UC3M in the line of Excellence of University Professors (EPUC3M23), and in the context of the V PRICIT (Regional Programme of Research and Technological Innovation). I.G.-A.P. was supported by the Ministerio de Ciencia, Innovación y Universidades (MCIU, Spain) through FPU Grant No. FPU18/02665.